Accepted Manuscript

Characterization of a novel Lytic Polysaccharide Monooxygenase from *Malbranchea cinnamomea* exhibiting dual catalytic behavior

Neha Basotra, Saurabh Sudha Dhiman, Dhruv Agrawal, Rajesh K. Sani, Adrian Tsang, Bhupinder S. Chadha

PII: S0008-6215(18)30738-9

DOI: https://doi.org/10.1016/j.carres.2019.04.006

Reference: CAR 7702

To appear in: *Carbohydrate Research*

Received Date: 19 December 2018

Revised Date: 27 March 2019

Accepted Date: 23 April 2019

Please cite this article as: N. Basotra, S.S. Dhiman, D. Agrawal, R.K. Sani, A. Tsang, B.S. Chadha, Characterization of a novel Lytic Polysaccharide Monooxygenase from *Malbranchea cinnamomea* exhibiting dual catalytic behavior, *Carbohydrate Research* (2019), doi: https://doi.org/10.1016/j.carres.2019.04.006.

Graphical abstract

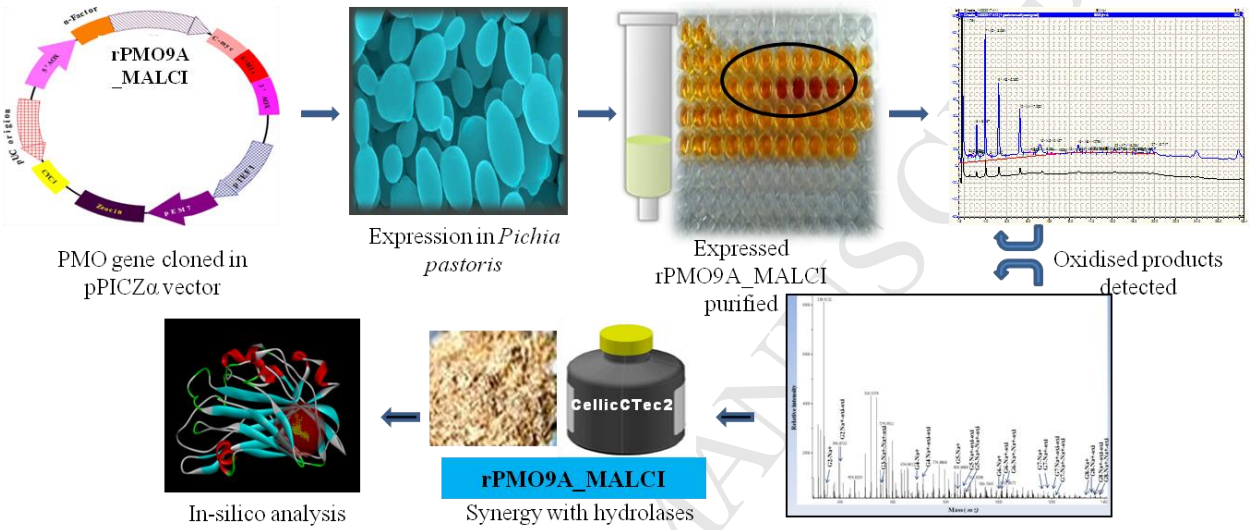

Running title: **A novel versatile LPMO from *Malbranchea cinnamomea* active on both cellulose and pure xylan**.

Characterization of a novel Lytic Polysaccharide Monooxygenase from *Malbranchea cinnamomea* exhibiting dual catalytic behavior

Neha Basotra[a‡], Saurabh Sudha Dhiman[b, c, d ‡], Dhruv Agrawal[a] , Rajesh K. Sani[b,c,d], Adrian Tsang[e] and Bhupinder S. Chadha[a,*]

[a]Department of Microbiology, Guru Nanak Dev University, Amritsar, Punjab 143005, India

[b]Department of Chemical and Biological Engineering, South Dakota School of Mines and Technology, Rapid City, SD 57701, USA

[c]Composite and Nanocomposite Advanced Manufacturing Center - Biomaterials [CNAM/Bio], Rapid City, SD 57701, USA

[d]BuG ReMeDEE Consortium, South Dakota School of Mines and Technology, Rapid City, SD 57701, USA

[e]Center for Structural and Functional Genomics, Concordia University, 7141 Sherbrooke Street, West, Montreal, Quebec H4B 1R6, Canada

Corresponding author:

*Bhupinder S. Chadha: chadhabs@yahoo.com

‡ Equal contribution by each author

Abstract

A novel Lytic Polysaccharide Monooxygenase (LPMO) family AA9 (PMO9A_MALCI) protein from thermophilic fungus *Malbranchea cinnamomea* was cloned and expressed in *Pichia pastoris*. The expressed protein was purified to homogeneity using ion exchange and hydrophobic interaction chromatography. SDS-PAGE analysis showed PMO9A_MALCI to be ~27 kDa protein. High performance anion exchange chromatography and mass spectrometry confirmed that purified protein was active against an array of cellulosic (avicel, carboxy methyl cellulose) and hemicellulosic (birch wood xylan, wheat arabinoxylan and rye arabinoxylan) substrates, releasing both oxidized and unoxidized cello-oligosaccharide and xylo-oligosaccharide products respectively. Presence of double oxidized products during mass spectrometric analysis as well as *in-silico* analysis confirmed that the expressed protein belongs to Type 3 LPMO family. Molecular dynamic simulations further confirmed the sharing of common amino acid residues conserved for catalysis of both cellulosic and hemicellulosic substrates which further indicates that both substrates are equally preferred. Enzymatic cocktails constituted by replacing a part of commercial cellulase CellicCTec2 with PMO9A_MALCI (9:1/8:2) led to synergistic improvement in saccharification of acid and alkali pretreated biomass. This is the first report on heterologous expression of LPMO from *M. cinnamomea*, exhibiting catalysis of cellulose and pure xylan.

Keywords: LPMO; heterologous expression; characterization; dual catalytic activity; docking; hydrolysis.

1. Introduction

Lytic Polysaccharide Mono-oxygenases (LPMOs) have garnered attention in recent times for their critical role in boosting the deconstruction of cellulosic substrates by puncturing the crystalline cellulose surface [1, 2, 3]. LPMOs are copper dependent mono-oxygenases which utilize molecular oxygen [4] or oxygen abstracted from H_2O_2 [5] to reduce the Cu^{2+} at their active site. This oxido-reduction process is followed by hydroxylation of substrate during cleavage of crystalline region of cellulose [6, 7]. For this cleavage process, role of an external source of electron such as ascorbic acid, reduced glutathione, gallate etc., is highly illustrious [8, 9]. However in some cases, extracellular cellobiose dehydrogenase (CDH), a natural redox enzyme co-secreted with LPMOs by several fungi, has been shown to serve as a source of electrons [3].

LPMOs are currently classified into auxiliary activity (AA) families 9, 10, 11, 13, 14 and 15 in the CAZy database [10]. The AA9 proteins were previously known as glycoside hydrolase family 61 (GH61) endoglucanase (EG) [11] owing to their weak activity against carboxymethyl cellulose (CMC) and were designated as EG-IV [12, 13]. Based on sequence variations, substrate recognition property and oxidation efficiency, AA9s are classified into Types 1, 2 and 3 [14]. Among classified types, oxidation of C1 (reducing end) and C4 (non-reducing end) of cellulose is governed by Type 1 and 2, respectively. Type 3 AA9 catalyzes the oxidation of both C1 and C4 of cellulosic substrates [15].

Structural elucidations and molecular analysis confirmed the presence of highly conserved histidine brace in all reported LPMOs [16]. Recent finding illustrated that the LPMO activities cover a broader range of substrates (cellulose, xyloglucan, xylans associated with cellulose etc.) [17,18]. However, no LPMO activity on pure xylan substrate has been reported till date. This paper reports the heterologous expression, purification and biochemical/*in-silico* characterization

of unique LPMO from thermophilic fungus, *M. cinnamomea*. The current study for the first time reports a Type 3 AA9 family protein from *M. cinnamomea* active against cellulosic, substituted and un-substituted xylan substrates.

2. Materials and methods

2.1. Microbial strain and sequence information

Previously isolated and identified thermophilic fungus *M. cinnamomea* was used for the current investigation [19]. *M. cinnamomea* culture was grown on CWR (cellulose, Wheat bran, Rice straw) medium containing a mixture of cellulose, wheat bran and rice straw (3:1:1) at 40ºC under shaking conditions (180 rpm) [20]. *E. coli* strain DH5α and *Pichia pastoris* strain X-33 (Invitrogen, Carlsbad, CA) were used as hosts for sub-cloning experiment and heterologous expression of PMO9A_MALCI protein, respectively.

A total of eight AA9 encoding genes were found in the genome sequence of *M. cinnamomea* (CBS 343.55) which is available at http://www.fungalgenomics.ca/wiki/Fungal_Genomes. For cloning and expression in *Pichia pastoris*, coding sequence of one of the LPMO (PMO9A_MALCI) having gene model ID Malci1p7_001540 was selected on the basis of presence of N-terminal histidine, a second conserved histidine and a Q/EXYXXC motif in the sequence **[21].**

2.2. Heterologous expression and enzyme assay

Forty eight hour grown mycelium (frozen using liquid N_2) was used to extract the total RNA from *M. cinnamomea* using TRIzol (Ambion). mRNA was recovered from total RNA, using maxi mRNA isolation kit (Invitrogen, USA) and was used as a template for complementary DNA synthesis using previously described method [22]. Specific forward (GAAGGTACCATGCTTCCGAACGCAGCTGG) and reverse

(CCGATCTAGAGAATCGCGGAAAACATCCGG) primers were used for the amplification of PMO9A_MALCI gene (restriction sites for *KpnI* and *XbaI* are underlined). Size of PCR product was confirmed through agarose gel electrophoresis (1% w/v agarose) and desired amplified product was eluted from gel using Gene clean®Turbokit (MP).

The purified PCR product was introduced into the vector pPICZαA between *Kpn*I and *Xba*I restriction sites under the control of *AOX1* promoter, yielding pPICZαA-PMO9A_MALCI fusion set. This fusion set was linearized using *Pme*I (New England BioLabs), transformed into *P. pastoris* X33 by electroporation (Invitrogen, Carlsbad, CA, USA) and plated onto YPDS (1% Yeast extract; 2% peptone; 2% dextrose; and 1M sorbitol) medium containing 100 µg mL^{-1} zeocin as a selectable marker. The resultant colonies were randomly picked and inoculated in 10 mL of BMGY medium (buffered minimal glycerol complex medium). The grown cells of *P. pastoris* harboring PMO9A_MALCI gene were harvested by centrifugation (10,000 *g*; 10 min; 4ºC) and resuspended in 50 mL of BMMY (buffered minimal methanol medium) and further incubated with methanol (1% v/v) feeding carried out at an interval of 24h. After 96h, the cells were pelleted by centrifugation (10,000 *g*; 10 min; 4°C) and liquid extract was considered as crude enzyme and assayed using fluorometric methodology using Amplex red and horseradish peroxidase (HRP) as described previously [23]. Enzymatic activity was also determined using 2% (w/v) CMC as substrate, a method well documented for purification and characterization of GH61 [12, 13].

The reaction was carried out using 0.5ml of suitably diluted PMO9A_MALCI enzyme and 0.5 ml of the substrate prepared in sodium citrate buffer (50 mM; pH 6.0) and incubated at 50°C for 30 min. The reaction was stopped by adding 3 ml DNS, followed by boiling for 10 min. The amount of reducing sugars released was quantified at 540 nm. One unit of enzyme activity was defined as

the amount of enzyme that released 1µmol of glucose equivalent per minute. The assay was performed in triplicates. **The protein content was determined using Lowry's method** [24].

2.3. Purification and characterization of PMO9A_MALCI

Two-stage purification strategy (anion exchange followed by hydrophobic interaction exchange) was applied to crude PMO9A_MALCI enzyme. Before column (HiTrap QXL, 5 mL column; GE healthcare, USA) loading, culture supernatant (500 mL) was precipitated using 80% (v/v) acetone (< 4^{o}C). Precipitates were harvested by centrifugation (8000 x g for 30 min) and the resultant pellet was dissolved in 10 mL of buffer A (Tris-HCl; 25 mM; pH 8.0). Sample protein (48.80 mg) was loaded onto the column and a linear salt gradient from 100% buffer A to 50% buffer B (buffer A with 1M NaCl) at a flow rate of 1 mL min^{-1} was used to elute the bound protein using AKTA prime fast protein liquid chromatography system (GE Healthcare, USA). Eluted fractions, positive for activity against CMC were pooled, concentrated (10 kDa; Amicon ultra filtration; Millipore, USA) and loaded onto 5 mL phenyl FF Sepharose column (GE Healthcare, USA) equilibrated with buffer A (50 mM sodium citrate;pH 6.0 and 1.7M ammonium sulphate). Bound protein was eluted using linear gradient formed using buffer B (50mM sodium citrate; pH 6.0). The active fractions were combined for characterization. The protein content in the crude extract and in the chromatographic fractions was determined using Lowry's method [24]. Protein purity was analyzed by 12% SDS-PAGE as described by Laemmli [25].

Substrate specificity of the purified PMO9A_MALCI was determined by incubating it with different polysaccharides (Phosphoric Acid Swollen Cellulose [PASC], avicel, β-barley glucan, carboxymethyl cellulose, Whatman filter paper no.1, hydroxyethyl cellulose, xyloglucan, lichenin, laminarin birchwood xylan, oat spelt xylan, rye arabinoxylan, larchwood xylan, beechwood xylan, wheat arabinoxylan [both low viscosity and high viscosity], 4-O-methyl

glucuronoxylan, debranched arabinan) . PASC was prepared as described by Wood and co-workers [26]. The reaction (1 ml) was prepared using equal volume of purified enzyme and substrate 2% (w/v) prepared in sodium citrate buffer (50 mM; pH 6.0) and 0.1ml of 1 mM ascorbic acid was also added as a source of electron. The reaction mixture was incubated at 50°C for 30 min. The reaction was stopped by adding 3 ml DNS, followed by boiling for 10 min [27]. The amount of reducing sugars released was quantified at 540 nm.

2.3.1 Determination of pH, temperature optima

A temperature range of 30-80ºC and pH 3.0-10.0 were used to determine the optimal parameters of the PMO9A_MALCI protein. The pH profile was determined using 50 mM sodium acetate (pH 3.0-5.0), 50 mM sodium citrate (pH 6.0), 50mM sodium phosphate (pH 7.0-8.0), 50 mM Tris HCl (pH 9.0) and 50 mM NaOH-Glycine (pH 10.0) as buffers. The thermostability of PMO9A_MALCI was determined by incubating the enzyme up to 72h at 50 and 60ºC and pH 5.0. 7.0 and 9.0; and subsequently assaying for residual enzyme activity.

2.3.2 Effect of metal ions

The purified enzyme was incubated for 30 min at room temperature in solutions of different metal ions ($CaCl_2$, $CoCl_2$, $CuCl_2$, $CuSO_4$, $FeCl_3$, $FeSO_4$, KCl, $MgCl_2$, $MgSO_4$, $MnCl_2$, $MnSO_4$, NaCl, $ZnCl_2$ and $ZnSO_4$ at 1 mM concentration) and different reagents (β-mercaptoethanol, dithiothreitol, EDTA, N-bromosuccinimide and SDS at 1% w/v). The residual activity was assayed thereafter using CMC as substrate.

2.3.3. Characterization of hydrolysis products by HPAEC and mass spectrometry

For analyzing the hydrolysis products, 2% (w/v) of the birchwood xylan, rye arabino xylan, oat spelt xylan, xyloglucan, carboxy methyl cellulose, lichenin and avicel were used. The reaction (2.0 mL) was set up in 15 mL glass vials along with 0.5 ml (0.534 mg) of purified

PMO9A_MALCI in presence/absence of ascorbic acid (1 mM) as electron donor [4] and incubated at 50ºC for 48 h under shaking conditions (200 rpm). Samples were drawn after 48h and the released reducing sugars were detected using dinitro salicylic acid (DNS) method. The hydrolysed oligosaccharides and their corresponding aldonic acid and C4-gemdiol forms, generated after the reaction, were analyzed using high-performance anion exchange chromatography coupled with amperometric detection (Dionex; HPAEC-PAD) as described by Forsberg et al [28]. The samples were diluted in water (1:10) and injected (10 µL) using a PA200 (Dionex) column employing gradient elution program of 35 min for the quantification of C1-oxidized gluco/xylo-oligosaccharides. In brief, 0– 21 min, linear gradient 0–0.25 M NaOAc; 21–25 min, linear gradient 0.25–1 M NaOAc; 25–28 min isocratic gradient 1 M NaOAc; followed by equilibration (7 min) of the column with the starting conditions were used. The hydrolysis products were identified on the basis of the elution profile of the xylo-oligosaccharide and cello-oligosaccharide mix used as standard. Expected masses of sodium-adducted oxidized gluco-oligosaccharides for substrates incubated with PMO9A_MALCI were computed according to the previous studies carried out by Isaken et. al., 2014 and Westereng et. al., 2015 [29, 30]. In addition, analysis of the products released during hydrolysis was carried out using Bruker micro TOF QII mass spectrometer in positive and negative ESI mode with capillary voltage of 4500 V at 180^{o}C. Sample (100 µL) prepared in combination of acetonitrile (3:7) and directly injected **(0.1 mL/min)** to the ion source of the spectrometer.

2.4 Enzyme preparation and biomass saccharification

To assess the hydrolytic potential and the degree of synergy of the PMO9A_MALCI with the commercial cellulases (CellicCTec2, Novozymes), the saccharification experiment was carried out using alkali and acid treated rice straw and sugarcane bagasse as described previously [31].

Saccharification reactions were performed in 5 mL glass vial that contained 1 mL reaction mixture prepared using 70 mg of pretreated substrate (7% w/v substrate loading), 900 µL citrate buffer (50 mM; pH 5.0) and 100 µL of suitably diluted CellicCTec2 (6.6 mg protein /g substrate) as benchmark control. To analyze the synergistic effect, 10 and 20 µL of the 100 µL benchmark enzyme was replaced with PMO9A_MALCI (that contained 3.4 mg protein/mL). The reaction was carried out in presence of ascorbic acid (1mM). The hydrolysis was carried out for 96h at 50^{o}C and released glucose was assayed using glucose oxidase peroxidase kit (Span Diagonostic, India). All the experiments were performed in triplicates.

2.5. Homology modeling and structural validation

The multiple sequence alignment for the PMO9A_MALCI protein was carried out using other LPMO orthologue sequences using Discovery Studio (DS) R2 (Accelrys Software Inc., San Diego, CA). Protein BLAST was performed to identify the closely matched entries followed by confirmation of the alignment for deletions and insertions into the structurally conserved regions. For homology model (HM) preparation, unanimously, the crystal structure of *Thermoascus aurantiacus* (3ZUD) (resolution 1.9 Å) was selected as the template. Protein health and validation was carried out using PROCHECK. The active site was identified using the **Protein Data Bank** (PDB) coordinates of 3ZUD. Quality of protein structure was determined through **Discrete Optimized Protein Energy** (DOPE) score in MODELER. The Root-Mean-Square-Deviation (RMSD) between the models and template was calculated via superimposition, and RMSD was 0.25 Å based on C-alpha atoms. The generated structure was improved by subsequent refinement of the loop conformations by assessing the compatibility of an amino acid sequence to known PDB structures.

206

207 *2.6. Molecular docking and energy analysis*

208 Hydrogen atoms were added to the model and minimized, followed by the overall validation of
209 the model using PROCHECK. Carboxymethyl cellulose (CMC) and birchwood xylan (BWX)
210 were docked into the selected active site pocket of PMO9A_MALCI model. Candidate poses
211 were then created using random rigid-body rotations followed by simulated annealing. The
212 structure of protein was subjected to energy minimization using CHARMm force field [32]
213 Based on DOPE score and **Probability Distribution Field** (PDF) energy values, candidate pose
214 was selected. The substrate orientation which gave the lowest interaction energy was selected for
215 further analysis [33].

216 **3. Results and discussion**

217 *3.1. Heterologous expression of PMO9A_MALCI*

218 Thermophilic fungal strain *M. cinnamomea*, previously characterized to secrete a significant level
219 of metal dependent GHs including LPMOs [34], was taken up as a source of LPMO. The genome
220 wide analysis confirmed that *M. cinnamomea* harbors eight AA9 genes. An open reading frame
221 encoding AA9 from *M. cinnamomea* was amplified using cDNA as template and designated as
222 PMO9A_MALCI. Size of the amplicon was found to be 747 bp (Fig S1).
223 The amplicon was cloned in-frame with the secretion signal (*S. cerevisiae* α-factor) into the
224 expression vector pPICZαA under the control of AOX1 promoter. The resultant plasmid was
225 transformed into *P. pastoris* (X33) by electroporation and plated onto YPDS/zeocin medium and
226 incubated at 30ºC for 72 h. Resultant 22 transformants were screened for the expression of AA9
227 on BMMY medium with 1% methanol (v/v) (added at 24 h intervals) under shaking conditions

for 120 h. The resultant culture extract of each transformant was assayed for LPMO activity using amplex red as described previously [23].

The Amplex Red method, that detects H_2O_2 as futile by-product in the reaction has been used to quantify LPMO activity in purified protein [23] However due to background alcohol oxidase in the parent *P. pastoris* strain, the method showed inconsistency and therefore, the clones were screened for AA9 activity using CMC as substrate. AA9 previously classified as GH61 with weak endoglucanase activity has been used to characterize purified GH61 from *Trichoderma reesei* using CMC [24]. The reducing sugars released were detected after incubation of 30 min using DNS. The maximal expression of AA9 was observed in clone 15 (412 units/L; Fig S2) and was chosen for further purification and characterization.

3.2. Characterization of purified PMO9A_MALCI

Purified PMO9A_MALCI appeared to have a significantly higher molecular mass (~27kDa) than that estimated from the amino acid sequence computed using expasy software tool (24.7 kDa, without signal peptide) and this may be attributed to glycosylation (Fig. 1). The glycosylation of LPMO's (MtLPMO9B and MtLPMO9C) cloned and expressed from a thermophilic fungus *Myceliophthora thermophila* have been reported recently [9]. However, MtLPMO9B and MtLPMO9C were glycosylated differentially with 13 and 5 glycosyl units attached, respectively in the mature protein.

The purified enzyme was found to be highly active under alkaline conditions (pH 8.0-10.0) with optimum activity (130% relative activity) at pH 9.0 when compared to that observed at pH 5.0 & 6.0 (Fig. S3a). The purified enzyme was optimally active at 60^{o}C, but activity decreased significantly at 70^{o}C and 80^{o}C (Fig.S3b). PMO9A_MALCI was found to be stable at 50^{o}C and 60^{o}C and pH 5.0, 7.0 and 9.0 (Fig S3c). The enzyme exhibited half life (t1/2) of 67.6, 55.18 and

72h at pH 5.0, 7.0 and 9.0 respectively at 50^{o}C whereas at 60^{o}C calculated t1/2 was 54.6, 55.1 and 75.9h at pH 5.0, 7.0 and 9.0 respectively. Owing to its relatively high thermostability, PMO9A_MALCI can be useful in formulating enzymes for efficient hydrolysis of lignocellulosics.

Pre-incubation of enzyme in presence of metal ion and other molecules showed (Fig. S4) Cu^{2+} to significantly improve (127% relative activity) the catalytic activity of the purified enzyme. This may be attributed to the fact that PMOs are the metalloenzymes which require Cu^{2+} as cofactors in the active site for oxidative cleavage [4]. Besides Cu^{2+}, other metal ions responsible for enhanced catalytic activity (relative activity) were Fe^{3+} (119%), Mn^{2+} (117%) and Co^{2+} (111%). Whereas, in case of metal dependent *Phanerocheate chrysogenum* (PcGH61D) positive modulation was only observed in presence of Cu^{2+} and Mn^{2+} [29]. In presence of bromosuccinimide, significant loss in the enzyme activity (16% residual) was observed in PMO9A_MALCI indicating the presence of tryptophan residues at the active site of enzyme [35].

3.3. Dual catalytic behavior of PMO9A_MALCI enzyme

The activity of purified PMO9A_MALCI was tested against different cellulosic and xylanolytic substrates and surprisingly pronounced higher activity against xylans (RAX, WAX, and BWX) when compared to glucan substrates was observed (Fig.2). The high preferential activity towards xylans, when compared to cellulosic substrates, makes PMO9A_MALCI, a unique candidate protein. Previous report in recent times claimed LPMO from *M. thermophila* as the first to show oxidative catalysis of xylan, but only when it is associated with regenerated cellulose (RAC), however no activity was observed in LPMO from *M. thermophila* when xylan was used as sole substrate [17]. Similarly, two AA14-LPMOs designated as xylan oxidases from *Pycnoporus coccineus* were reported to cleave xylan coated cellulose fibers **[36]** but not pure xylans.

Therefore, observed dual catalytic behavior of PMO9A_MALCI against a wide array of xylan substrates as well as avicel, PASC, CMC, filter paper, β barley glucan (which contain mixed β1-3 and 1-4 linkages), laminarin and lichenin shows versatility of this LPMO. The LPMO from *Gloephylum trabeum Gt*LPMO9A-2 has been previously reported to be active on cellulose, carboxymethyl cellulose and xyloglucan [18].

3.4. Saccharification product analysis using HPAEC and MS

To analyze the oxidized/hydrolysed products formed as a result of PMO9A_MALCI activity on natural xylan substrates (birchwood xylan, rye arabinoxylan) and cellulose substrates (CMC, avicel, lichenin and xyloglucan), hydrolysis was carried out for 48 h in presence/absence of ascorbic acid and the enzyme showed high preference for RAX > BWX > CMC > lichenin > avicel as substrates. Expectedly the observed activities were higher in presence of reductant ascorbic acid when compared to in its absence (Fig. 3). The HPAEC profile (Fig. S5) of the BWX clearly shows the presence of xylobiose, xylotriose, xylotetraoase, xylyopentose as major hydrolysis products with decreasing intensity in that order. In addition oxidized products were observed to be eluted between 20-29 minutes as also observed previously [29, 30]. Due to absence of standards for HPAEC and moreover C4 oxidised sugars are difficult to analyze using HPAEC due to their on column decomposition in the presence of alkali [37], identification process of oxidized products was carried out using mass spectroscopy (MS). The MS analysis clearly showed the presence of oligosaccharides and oxidized products (DP2 to DP8). The results in **Table 1** confirmed the presence of sodium adducts of oxidized (+16), double oxidized and unoxidized products of xylo-oligosaccharides (X2-X8) in the sample of BWX (Fig. S6) and RAX. Similarly, oxidized and unoxidized cello-oligosaccharides (G2-G8) were also observed in the hydrolysate derived from CMC (Fig.S7 and **Table 2**) and avicel (**Table 2**). Both C1 and C4

297 oxidised sugars, for example aldonic acid+gemdiol (M+32) and 1,5 delta
298 lactone+gemdiol/aldonic acid+4-ketoaldose (M+14) corresponds to 883 and 865 m/z values,
299 respectively [38]. The presence of double oxidized (C1/C4) products suggested that
300 PMO9A_MALCI may belong to Type 3 AA9 and coincides with the properties exhibited by AA9
301 from *Thermoascus aurantiacus* and *Neurospora crassa* [7, 8].

302 3.5. *Synergistic role of PMO9A_MALCI in biomass saccharification*

303 Four different pretreated biomass samples i.e., acid and alkali treated rice straw (AcRS and AlRS)
304 and bagasse (AcBG and AlBG) were used to evaluate the boosting effect of PMO9A_MALCI
305 when supplemented to benchmark cellulase preparations CellicCtec2 by replacing either 1-part
306 (9:1) or 2 parts (8:2) of enzyme with purified recombinant PMO9A_MALCI. Results in Fig. 4
307 showed when compared to benchmark an enhanced level of hydrolysis of acid and alkali treated
308 rice straw (28.7 and 24.8%) respectively, when a cocktail of CellicCTec2 and PMO9A_MALCI
309 was used in 9:1 ratio. Similarly, 22.7 and 13.28% improvement in release of sugars was observed
310 when AcBG and AlBG were used as substrates (9:1). However, the boosting effect of
311 PMO9A_MALCI in release of sugars was more pronounced (35.7, 36.65, 28.9 and 21.4 % for
312 AcRS, AlRS, AcBG and AlBG respectively) in a cocktail containing CellicCtec2 and
313 PMO9A_MALCI in 8:2 ratio when compared to benchmark. The improved levels of hydrolysis
314 of different substrates using cocktails of cellulases with PMO9A_MALCI show its importance in
315 formulating cocktails applicable to different lignocellulosic substrates.

316 *3.5.Secondary structure and homology modeling of PMO9A_MALCI*

317 For homology modeling and structural superimposition, crystal structures of thermophilic fungi
318 *Thermoascus* sp. (ID: 3ZUD) and *Trichoderma reesei* (PDB ID: 2VTC_A) were aligned with the
319 sequence of PMO9A_MALCI protein. The 3D homology model (HM) and structural

superimposition is shown in Fig 5a and 5b, respectively. The value of verified score (104) was comparable to verified expected high score (103), confirmed the validity of the generated HM [39]. Comparison of active site and structural superimposition analysis revealed the similar active site environment. The active site pocket interacting with both the substrates (CMC and BWX) includes 3 residues each. Interestingly 2 residues viz. N124 and G126 were common for active sites of both types of substrates.

Calculated Ramachandran's plot (Fig. S7) confirmed the presence of 96.0% residues (215) in favored region indicating the accuracy of backbone dihedral angles followed by presence of nearly 2.2% residues [5] in allowed region. Only 4 residues (1.8%) were present in the outlier region. Combined presence of more than 98% residues in favored and allowed region confirmed the validity of protein folds and overall structure of the model [40]. It is generally accepted that a score close to 100% depicts good stereochemical quality of the model. Therefore, these results suggesting 98.0% score indicate that the predicted model is of good quality.

3.6.Molecular docking and interaction analysis

Based on the minimum PDF energy, HM was selected for molecular docking analysis. For molecular docking, Momany Rone and CHARMM forcefield approaches were followed for applying the partial charge and forcefield on xylan molecule. Observed PDF physical energy and RMSD value for the selected pose of birchwood xylan were -739kcal/mol and 0.407, respectively. Binding of xylan molecule was tightly regulated by H-bonds with the active site residues. Bond distance values were less than 5Å for all the active site residues. For efficient substrate catalysis, bonds exhibiting the distance values less than 5Å are crucial for enzymatic reaction [41].

Hydrogen atoms of H87 was interacting with O5 (sp^3) and O2 (sp^3) of the BWX through H-bonds **(Fig. 6)**. Likewise, O4 (sp^3) of xylan was interacting with H1 (2.84Å) of N124 via conventional H-bond. This conventional H-bond exhibited a DHA angle of 106.5^o in which H22 of residue was acting as the donor and sp^3 hybridized O4 of substrate was functioning as recipient. With other active sites residue, H13 of substrate was acting as donor and involved in carbon-hydrogen bond (2.50Å) with sp^2 hybridized O-atom of G126 (**Fig. 6**; distance with blue background), resulted in the formation of total 4 H-bonds. Observation of high number of H-bond (like current study) by three or less residues within active site is very rare property of any enzyme [42].

Interaction of substrate with multiple O-atoms of active site residues, restrict any change in confirmation after binding and thus catalyze the substrate efficiently. Tight regulation of xylan within the active site might be the reason for observed activity of PMO9A_MALCI protein against pure xylan as substrate. Arrangement of different residues involved in binding and substrate catalysis was also studied. Presence of polar E84 contributes towards stability of active site via formation of salt-bridges. These salt-bridges involve strong interactions with closely placed histidine residues (H86, H87) of the LPMO and thus govern the catalysis due to their interaction with the hydrophilicity of the protein and are also crucial for the stability of active site pocket may govern the interaction of docked substrate with other polar and charged atoms of the birchwood xylan. Presence of hydrophilic residues viz. S85, Y127 is also important for substrate oxidation because of their characteristic property of acting as proton-donor [43]. Y127 also contributes N-atom to binding site which is crucial for binding of non-protein atoms via stacking interactions [44].

Observed PDF physical energy for docked CMC was similar to the value noted for BWX. This might be the reason for similar catalytic efficiency exhibited by LMPO for both the substrate. For

365 docked CMC, molecular oxygen atom of P125 interacting with two hydrogen atoms viz 13 and 20
366 via H-bonds **(Fig. 7)**. A bond angle of 61.2º was maintained by H13 and H20 of CMC with O-
367 atom of P125 **(Fig. 7)**. **Molecular dynamic** (MD) simulation confirmed the distortion of active
368 site with any variation in these bond angles through *in-silico* mutagenesis (data not given). Thus,
369 confirmed the vital role of P125 in the oxidation reaction performed by PMO9A_MALCI protein.
370 Sp^3 hybridized O3 of CMC was interacting with H22 and H23 of N124 through H-bonds. Though
371 D203 was in the proximity of the active site but docked molecules were interacting with less
372 affinity compared to other active site residues (data not given). As for docked CMC, the non-bond
373 ligand interactions beyond 5Å radius were not analyzed for molecular interactions. LPMOs are
374 metallo-proteins reported for mononuclear copper [45].
375 Presence of common residues (S85, H87, N124, G126) in binding site of Type 3-LPMO protein
376 from *M. cinnamomea* is crucial for the dual catalytic behavior. However, presence of more
377 defined and large (size-wise) active site for CMC illustrates the preference of PMO9A_MALCI
378 protein for CMC over BWX. Presence of G126 in the binding pocket may govern the flexibility
379 exhibited by PMO9A_MALCI protein for catalysis of dual substrates. Close placement of Cu^{2+}
380 within the active site of the PMO9A_MALCI protein (for both the substrates) may create steric
381 hindrance and may govern the non-bond ligand interaction (data not given). However, to confirm
382 the redox state and interactions of Cu^{2+} with metal-binding site residues, in-depth analysis is
383 required (separate manuscript underway).
384 Homology model of PMO9A_MALCI using the crystal structure of *T. aurantiacus* (3ZUD) as a
385 template, the overall shape of the substrate binding pocket (SBP) of PMO9A_MALCI was found
386 to be similar to those of the *T. aurantiacus* and *Hypocrea jecorina*. Homology modeling of the
387 three-dimensional structure indicated that the surface-exposed H86 and D203 in the catalytic

cavity play major roles in the oxidation of substrates (data not given). The substrate birch wood xylan binds to the H86 exposed on the surface, and not directly to the metal ion. H86 has been suggested to be a primary electron acceptor, and positioned optimally to interact with substrate because of its easy access to the molecule's surface. Another interesting residue in PMO9A_MALCI structure is D203. This hydrophilic residue in the cavity plays an important role in substrate oxidation by accepting a proton from the substrate [10]. Ligand entropy for BWX and CMC was computed as -17.56 and -17.95 Kcal/mol, respectively (Table S1).

4. Conclusions

Recombinant PMO9A_MALCI can be regarded as distinct and versatile LPMO yet reported with broad substrate specificity. Mass spectral analysis of recombinant protein and gene sequence analysis confirmed the classification of PMO9A_MALCI as Type 3 AA9s, catalyzing both C1 and C4 oxidations. In-depth analysis of active site environment, metal ion interactions will provide crucial details in comprehending the oxidation mechanism followed by other oxidative enzyme systems. Improved saccharification efficiency of PMO9A_MALCI in conjunction with CellicCTec2 confirmed the transformative role offered by LPMO for sustainable biorefinery applications.

Acknowledgement

This research was supported by the Department of Biotechnology, India, Project (BT/PR 15271/PBD/26/509/2015). Research fellowship provided to Neha Basotra in the form of IUSSTF-DBT B-ACER award is highly acknowledged. Authors also acknowledge the financial support provided by National Science Foundation and South Dakota Governor's Office of Economic Development (USA). In addition, research support from the Department of Chemical

and Biological Engineering at the South Dakota School of Mines and Technology is also acknowledged.

Competing interests

The author(s) declare no competing interests.

References

1. I. Morgenstern, J. Powlowski, A. Tsang, Fungal cellulose degradation by oxidative enzymes: from dysfunctional GH 61 family to powerful lytic polysaccharide monooxygenase family, Brief. Funct. Genomics. 13 (2014) 471-481.
2. K.S. Johansen, Discovery and industrial applications of lytic polysaccharide mono-oxygenases, Biochem. Soc. Trans. 44 (2016) 143–149.
3. G. Vaaje-Kolstad , B. Westereng, S.J. Horn, Z. Liu, H. Zhai, M. Sorlie, V.G.H. Eijsink, An oxidative enzyme boosting the enzymatic conversion of recalcitrant polysaccharides, Science. 330 (2010) 219–222.
4. S. Kim, J. Stahlberg, M. Sandgren, R.S. Paton, G.T. Beckham, Quantum mechanical calculations suggest that lytic polysaccharide monooxygenases use a copper-oxyl, oxygen-rebound mechanism, Proc. Natl. Acad. Sci. USA. 111 (2014) 149–154.
5. B. Bissaro, A.K. Rohr, M. Skaugen, Z. Forsberg, S.J. Horn, G. Vaaje-Kolstad, Fenton-type chemistry by a copper enzyme: molecular mechanism of polysaccharide oxidative cleavage, bioRxiv. (2016) doi: 10.1101/097022.
6. S.J. Horn, G. Vaaje-Kolstad, B. Westereng, V.G. Eijsink, Novel enzymes for the degradation of cellulose, Biotechnol. Biofuels. 5 (2012) 45.

7. C.M. Phillips, W.T. Beeson, J.H. Cate, M.A. Marletta, Cellobiose dehydrogenase and a copper-dependent polysaccharide monooxygenase potentiate cellulose degradation by *Neurospora crassa*, ACS. Chem. Biol. 6 (2011)1399–1406.
8. R.J. Quinlan, M.D. Sweeney, L. Lo Leggio, H. Otten, J.C. Poulsen, K.S. Johansen, Insights into the oxidative degradation of cellulose by a copper metalloenzyme that exploits biomass components, Proc .Natl. Acad. Sci. USA. 108 (2011) 15079–15084.
9. M. Frommhagen, M.J. Koetsier, A.H. Westphal, J. Visser, S.W.A. Hinz, J.P. Vincken, Lytic polysaccharide monooxygenases from *Myceliophthora thermophila* C1 differ in substrate preference and reducing agent specificity, Biotechnol. Biofuels. 9 (2016) 186.
10. T. Tandrup , K.E.H. Frandsen, K.S. Johansen, J.G. Berrin, L.L. Leggio, Recent insights into lytic polysaccharide monooxygenases (LPMOs), Biochem. Soc. Trans. 46 (2018) 1431-1447.
11. P. Busk, L. Lange, Classification of fungal and bacterial lytic polysaccharide monooxygenases, BMC. Genomics. 16 (2015) 368.
12. M. Saloheimo, T. Nakari-Setala, M. Tenkanen, M. Penttila, cDNA cloning of a *Trichoderma reesei* cellulase and demonstration of endoglucanase activity by expression in yeast, Eur. J. Biochem. 249 (1997) 584–591.
13. J. Karlsson, M. Saloheimo, M. Siika-Aho, M. Tenkanen, M. Penttila, F. Tjerneld, Homologous expression and characterization of Cel61A [EG IV] of *Trichoderma reesei*, Eur. J. Biochem. 268 (2001) 6498-6507.
14. W.T. Beeson, C.M. Phillips, J.H. Cate, M.A. Marletta, Oxidative cleavage of cellulose by fungal copper-dependent polysaccharide monooxygenases, J. Am. Chem. Soc. 134 (2012) 890–892.

15. V.V. Vu, W.T. Beeson, C.M. Phillips, J.H. Cate, M.A. Marletta, Determinants of regioselective hydroxylation in the fungal polysaccharide monooxygenases, J. Am. Chem. Soc. 136 (2014) 562–565.

16. F.L. Aachmann, M. Sørlie, G. Skjåk-Braek, V.G.H. Eijsink, G. Vaaje-Kolstad, NMR structure of a lytic polysaccharide monooxygenase provides insight into copper binding, protein dynamics, and substrate interactions, Proc. Natl. Acad. Sci. USA. 109 (2012) 18779–18784.

17. M. Frommhagen, S. Sforza, A.H. Westphal, J. Visser, S.W. Hinz, M.J. Koetsier, Discovery of the combined oxidative cleavage of plant xylan and cellulose by a new fungal polysaccharide monooxygenase, Biotechnol. Biofuels, 8 (2015) 101.

18. Y. Kojima, A. Várnai, T. Ishida, N. Sunagawa, D.M. Petrovic, K. Igarashi, J. Jellison, B. Goodell, G. Alfredsen, B. Westereng, V.G.H. Eijsink, M. Yoshida, A Lytic Polysaccharide monooxygenase with broad xyloglucan specificity from the brown-rot fungus *Gloeophyllum trabeum* and its action on cellulose-xyloglucan complexes, Appl. Environ. Microbiol. 82 (2016) 6557-6572.

19. C. Mahajan, B.S. Chadha, L. Nain, A. Kaur, Evaluation of glycosyl hydrolases from thermophilic fungi for their potential in bioconversion of alkali and biologically treated *Parthenium hysterophorus* weed and rice straw into ethanol, Bioresour. Technol. 163 (2014) 300-307.

20. R. Rai, B. Kaur , S. Singh, M. Di Falco, A. Tsang, B.S. Chadha BS, Evaluation of secretome of highly efficient lignocellulolytic *Penicillium* sp. Dal 5 isolated from rhizosphere of conifers, Bioresour. Technol. 216 (2016) 958–967.

21. G. Jagadeeswaran, L. Gainey, R. Prade, A.J. Mort, A family of AA9 lytic polysaccharide monooxygenases in *Aspergillus nidulans* is differentially regulated by multiple substrates and at least one is active on cellulose and xyloglucan. Appl. Microbiol. Biotechnol. 100 (2016) 4535-4547.

22. P. Carninci, Y. Nishiyama, A. Westove, M. Itoh, S. Nagaoka, N. Sasaki, Y. Okazaki, M. Muramatsu, Y. Hayashizaki, Thermostabilization and thermoactivation of thermolabile enzymes by trehalose and its application for the synthesis of full length cDNA , Proc. Nat. Acad. Sci. U.S.A. 95 (1998) 520-524.

23. R. Kittl , D. Kracher, D. Burgstaller, D. Haltrich, R. Ludwig, Production of four *Neurospora crassa* lytic polysaccharide monooxygenases in *Pichia pastoris* monitored by a fluorimetric assay, Biotechnol. Biofuels. 5 (2012) 79.

24. O.H. Lowry, N.J. Rosebrough, A.L. Farr, R.J. Randall, Protein measurement with the folin phenol reagent, J. Biol. Chem. 193 (1951) 265–275.

25. U.K. Laemmli, Cleavage of structural proteins during the assembly of head of bacteriophage T4, Nature. 227 (1970) 680–685.

26. T.M. Wood, Preparation of crystalline, amorphous and dyed cellulase substrates, Methods. Enzym. 160 (1988) 19–25.

27. G.L. Miller, Use of dinitrosalicylic acid reagent for determination of reducing sugar, Anal. Chem. 31(1959) 426–428.

28. Z. Forsberg, G. Vaaje-Kolstad, B. Westereng, A.C. Bunæs, Y. Stenstrøm, A. Mackenzie, M. Sørlie, S.J. Horn, V.G.H. Eijsink, Cleavage of cellulose by a CBM33 protein, Protein Sci. 20 (2011) 1479-1483.

29. T. Isaksen, B. Westereng, F.L. Aachmann, J.W. Agger, D. Kracher, R. Kittl, A C4-oxidizing lytic polysaccharide monooxygenase cleaving both cellulose and cello-oligosaccharides, J. Biol. Chem. 289 (2014) 2632–2642.

30. B. Westereng, D. Cannella, J. Wittrup Agger, H. Jorgensen, M. Larsen Andersen, V.G. Eijsink, C. Felby, Enzymatic cellulose oxidation is linked to lignin by long-range electron transfer, Sci. Rep. 5 (2015) 18561.

31. N. Basotra, B. Kaur, M. Di Falco, A. Tsang, B.S. Chadha, *Mycothermus thermophilus* (Syn. *Scytalidium thermophilum*): Repertoire of a diverse array of efficient cellulases and hemicellulases in the secretome revealed, Bioresour. Technol. 222 (2016) 413-421.

32. B.R. Brooks, R.E. Bruccoleri, B.D. Olafson, D.J. States, S.A. Swaminathan, M. Karplus, CHARMM: A program for macromolecular energy, minimization, and dynamics calculations, J. Comp. Chem. 4 (1983) 187-217.

33. M.Y. Shen, A. Sali, Statistical potential for assessment and prediction of protein structures, Protein. Sci. 15 (2006) 2507-2524.

34. C. Mahajan, N. Basotra, S. Singh, M. Di Falco, A. Tsang, B.S. Chadha, *Malbranchea cinnamomea*: A thermophilic fungal source of catalytically efficient lignocellulolytic glycosyl hydrolases and metal dependent enzymes, Bioresour. Technol. 200 (2016) 55-63.

35. M. Sharma, B.S. Chadha, H.S. Saini, Purification and characterization of two thermostable xylanases from *Malbranchea flava* active under alkaline conditions, Bioresour. Technol. 101 (2010) 8834–8842.

36. M. Couturier, S. Ladevèze, G. Sulzenbacher, L. Ciano, M. Fanuel, C. Moreau, A. Villares, B. Cathala, F. Chaspoul, K.E. Frandsen, A. Labourel, I. Herpoël-Gimbert,

S. Grisel, M. Haon, N. Lenfant, H. Rogniaux, D. Ropartz, G.J. Davies, M.N. Rosso, P.H. Walton, B. Henrissat, J.G. Berrin, Lytic xylan oxidases from wood-decay fungi unlock biomass degradation. Nat, Chem. Biol. (2018) doi:10.1038/nchembio.2558.

37. B. Westereng, M.O, Arntzen, F.L. Aachmann, A. Varnai, V.G.H. Eijsink, J.W. Agger, Simultaneous analysis of C1 and C4 oxidized oligosaccharides, the products of lytic polysaccharide monooxygenase acting on cellulose, J. of Chromatogr. A. 1445 (2016) 46-54.
38. M. Bey, S. Zhou, L. Poidevin, B. Henrissat, P.M. Coutinho, J.G. Berrin, J.C. Sigoillota, Cello-oligosaccharides oxidation reveals differences between two lytic polysaccharide monooxygenases (Family GH61) from *Podospora anserine*, Appl. Environ. Microbiol. 79 (2013) 488-96.
39. L. Bordoli, T. Schwede, Automated protein structure modeling with swiss-model workspace and the protein model portal, Methods. Mol. Biol. 857 (2012)107-136.
40. S.C. Lovell, I.W. Davis, W.B. Arendall III, P.I.W. de Bakker, J.M. Word, M.G. Prisant, J.S. Richardson, D.C. Richardson, Structure validation by C-alpha geometry: phi-psi and C-beta deviation, Proteins: Structure, Function & Genetics. 50 (2002) 437-450.
41. E. Notomista, V. Cafaro, G. Bozza, A. Di Donato, Molecular determinants of the regioselectivity of toluene/o-xylene monooxygenase from *Pseudomonas* sp. strain OX1, *Appl.* Environ. Microbiol. 75 (2009) 823-836.
42. P.A. Frey, Strong hydrogen bonding in molecules and enzymatic complexes, Magn. Reson. Chem. 39 (2001) S190–S198.
43. R.L. Levine, L. Mosoni, B.S. Berlett, E.R. Stadtman, Methionine residues as endogenous antioxidants in proteins, Proc. Natl. Acad. Sci. 93 (1996) 15036-15040.

546 44. M.L. Khamis, J.R. Casas-Finet, A.H. Maki, Stacking interactions of tryptophan residues
547 and nucleotide bases in complexes formed between *Escherichia coli* single-stranded DNA
548 binding protein and heavy atom-modified poly (uridylic) acid. A study by optically
549 detected magnetic resonance spectroscopy, J. Biol. Chem. 262 (1987) 1725-1733.
550 45. D. Kracher, M. Andlar, P.G. Furtmüller, R. Ludwig, Active-site copper reduction
551 promotes substrate binding of fungal lytic polysaccharide monooxygenase and reduces
552 stability. J. Biol. Chem. 293 (2018) 1676-1687.
553
554

555 **Figure legends:**

556

557 **Figure 1:** SDS–PAGE of purified PMO9A_MALCI.

558 Lane M: protein ladder (Precision PLUS Protein standards, BIORAD); Lane 1: purified
559 PMO9A_MALCI (~27 kDa); and Lane 2: crude extract showing expressed PMO9A_MALCI

560

561 **Figure 2:** Substrate specificity of the purified PMO9A_MALCI.

562 BWX: birch wood xylan; RAX: rye arabinoxylan; WAX: wheat arabino -xylan; OSX: oat spelt xylan; BEEWX:
563 beech wood xylan; LWX: larch wood xylan; 4-O-MGUX: 4-O-methyl-D-glucurono-D xylan; DBA: debranched
564 arabinan. CMC: carboxy methyl cellulose; PASC: phosphoric acid swollen cellulose; FP: filter paper; HEC:
565 hydroxyethyl cellulose; Bars represent mean± SE (n=3)

566

567 **Figure 3:** Amount of reducing sugars released during hydrolysis of natural substrates using
568 purified PMO9A_MALCI both in the presence and absence of ascorbic acid. BWX: birchwoodxylan;
569 RAX: rye arabinoxylan; CMC: carboxymethyl cellulose; Bars represent mean± SE (n=3)

570

571 **Figure 4:** Amount of glucose released (mg/ml) after saccharification (96h) of differently treated
572 rice straw and bagasse using cocktails containing CellicCTec2 and PMO9A_MALCI in 9:1 and
573 8:2 ratios.

574 AcRS: Acid treated Rice Straw; AlRS: Alkali treated Rice Straw; AcBG: Acid treated Bagasse; AlBG: Alkali treated
575 Bagasse; Bars represent mean± SE (n=3)

576 **Figure 5:** 3D (a) homology model and (b) structural superimposition of LMPO protein from *M.*
577 *cinnamomea.* Structural superimposition with ***Thermoascus aurantiacus*** (3ZUD, Blue colored)

578 and ***Hypocrea jecorina*** (2VTC, Yellow) confirmed the classification of PMO9A_MALCI as
579 Type 3 LPMO
580
581 **Figure 6:** Molecular docking analysis of birchwood xylan (BWX) as substrate with the active site
582 residues of PMO9A_MALCI protein
583 Bond distance and bond angle values are given in Å.
584
585 **Figure 7:** Molecular docking analysis of CMC as substrate within the active site residues of
586 PMO9A_MALCI protein.
587 Bond distance and bond angle values are given in Å.
588
589
590
591
592
593
594
595
596
597
598
599
600

601

602

603

604 **Fig. 1**

605

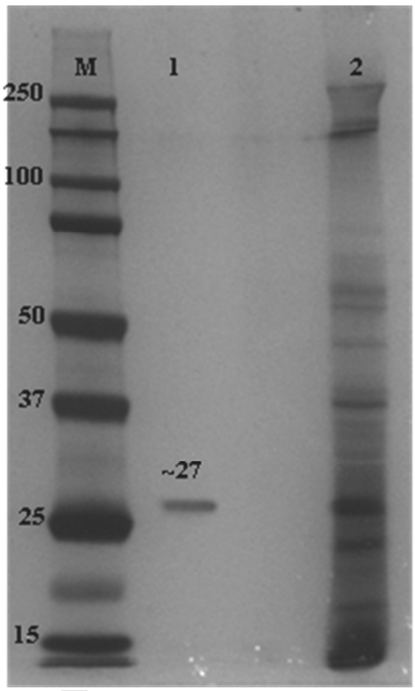

606

607

608

609 **Fig. 2**

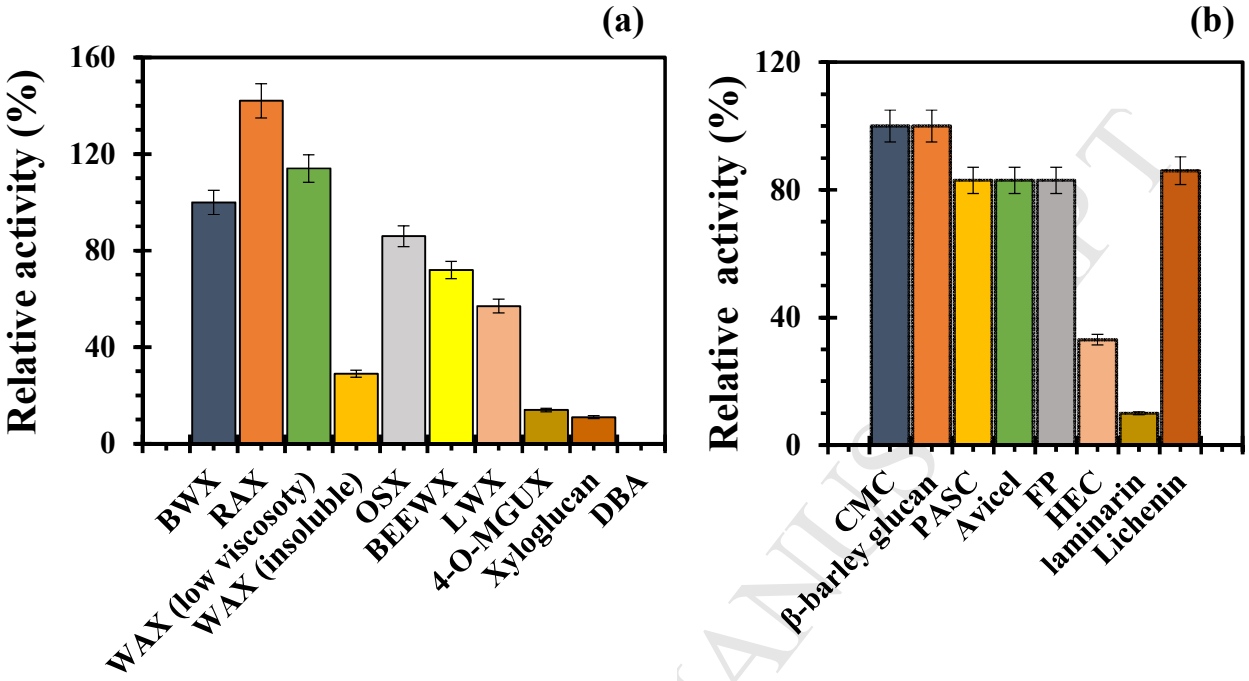

610

611

612
613
614
615
616
617
618
619
620
621
622
623
624
625
626
627
628
629
630
631
632
633
634

635 **Fig. 3**

636

637

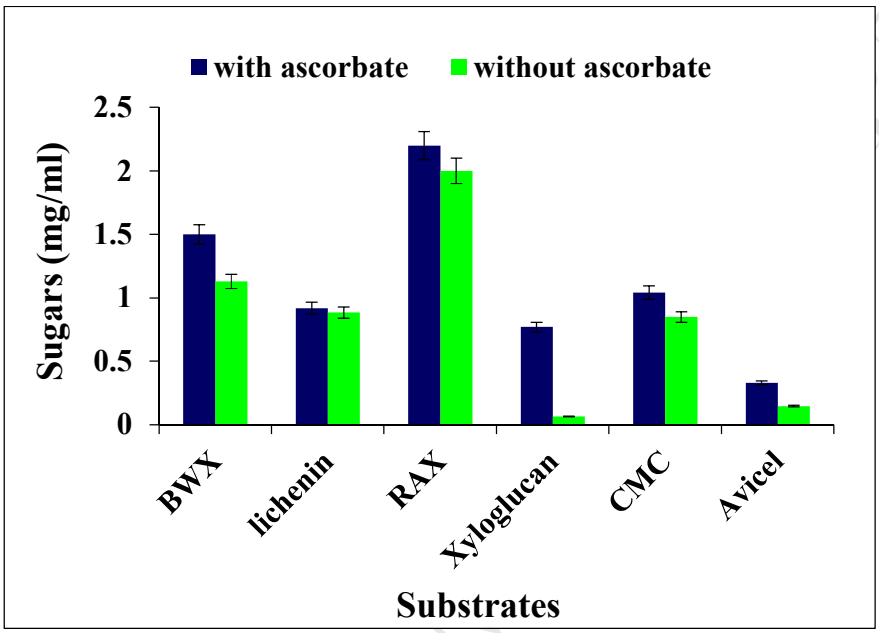

638

639

640

641

642

643

644

645

646

647

648

649

650 **Fig. 4**

651

652

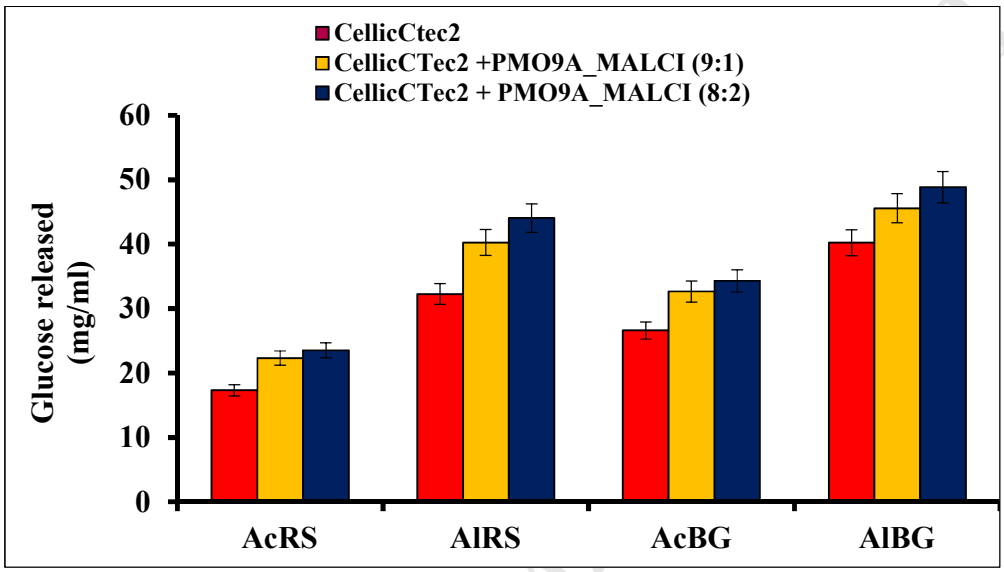

653

654

655

656

657

658

659

660

661

662

663

664

665

666

667

Fig. 5

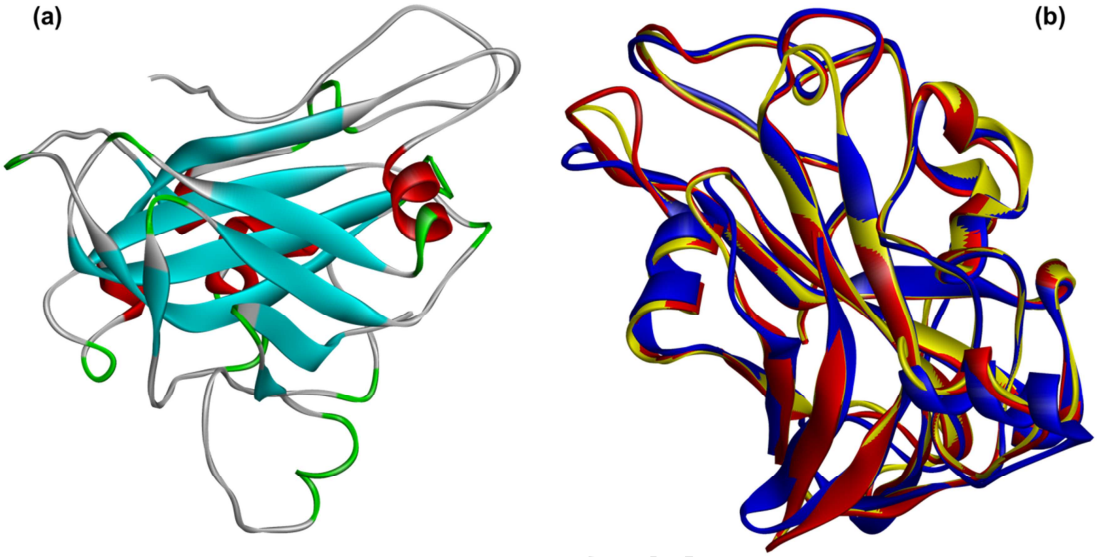

686

687 **Fig. 6:**

688

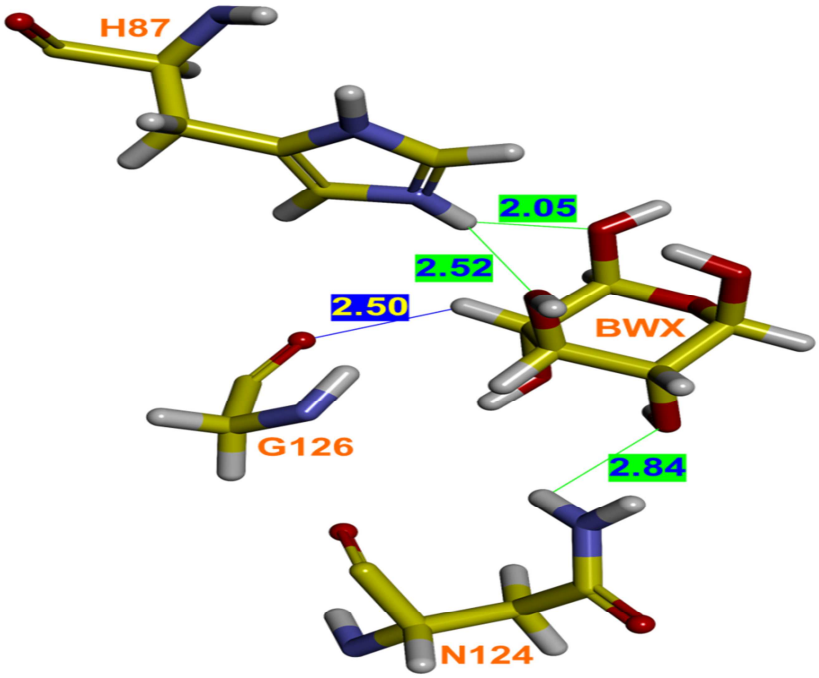

689

690

691

692

693

694

695

696

697

698

699

700

701

Fig. 7:

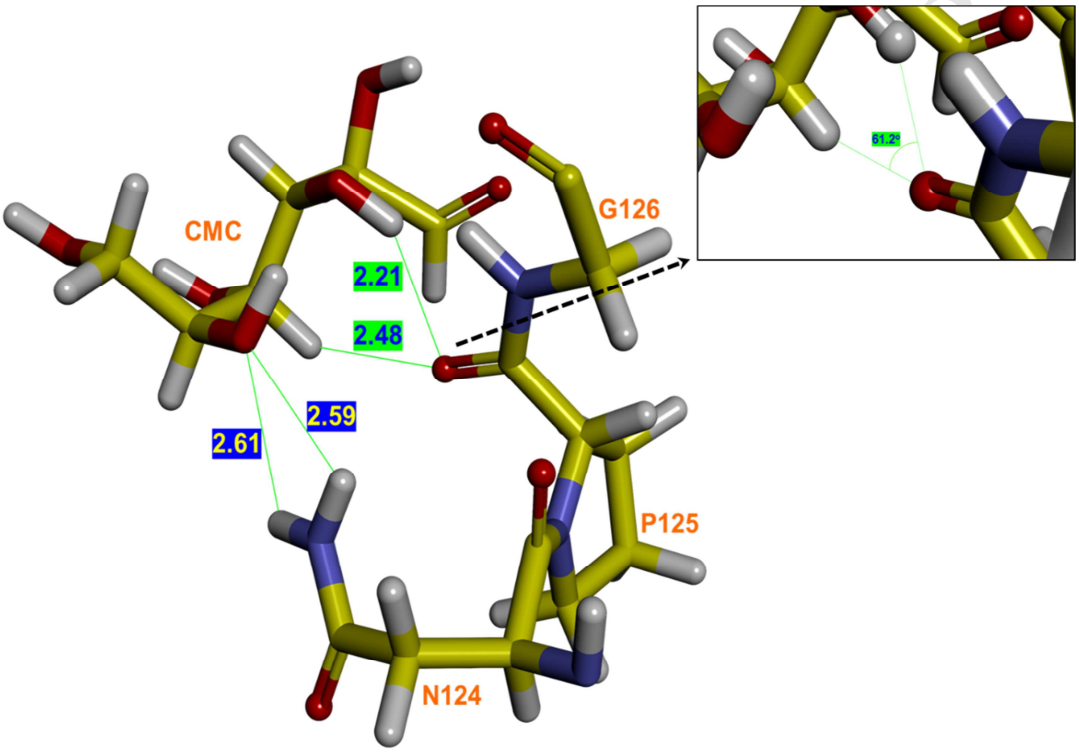

715 **Table 1.** Mass-spectroscopy based analysis of hydrolysis products obtained from Rye Arabino
716 Xylan (RAX) and Birch Wood Xylan (BWX) using purified PMO9A_MALCI.

717

Pentose Products (m/z)	Structure	RAX	BWX
DP2			
305	X2-Na+	Present	Present
321	X2-Na+-oxi	ND	Present
343	X2-Na+-Na+-oxi	ND	Present
337	X2 Na+-oxi-oxi	ND	ND
DP3			
437	X3-Na+	Present	Present
453	X3-Na+-oxi	Present	Present
475	X3-Na+-Na+-oxi	ND	ND
469	X3 Na+-oxi-oxi	ND	Present
DP4			
569	X4-Na+	Present	Present
585	X4-Na+-oxi	ND	Present
607	X4-Na+-Na+-oxi	ND	Present
601	X4 Na+-oxi-oxi	ND	Present
DP5			
701	X5-Na+	Present	Present
717	X5-Na+-oxi	Present	Present
739	X5-Na+-Na+-oxi	Present	Present
733	X5 Na+-oxi-oxi	Present	Present
DP6			
833	X6-Na+	Present	Present
849	X6-Na+-oxi	Present	Present
871	X6-Na+-Na+-oxi	Present	Present
849	X6 Na+-oxi-oxi	Present	Present
DP7			
965	X7-Na+	Present	Present
981	X7-Na+-oxi	Present	Present
1003	X7-Na+-Na+-oxi	Present	Present
997	X7 Na+-oxi-oxi	Present	Present
DP8			
1097	X8-Na+	Present	Present
1113	X8-Na+-oxi	Present	Present
1135	X8-Na+-Na+-oxi	Present	Present
1129	X8 Na+-oxi-oxi	Present	Present

718

719 RAX: Rye Arabinoxylan; BWX: Birch Wood Xylan; DP: Degree of Polymerization; X: Xylo-oligosaccharides; Na+:
720 sodium adduct; ND: not detected

721 **Table2.** Mass-spectroscopy based analysis of hydrolysis products obtained from Carboxy Methyl
722 Cellulose (CMC) and avicel using purified PMO9A_MALCI.
723

Hexose Products (m/z)	Structure	CMC	Avicel
DP2			
365	G2-Na+	Present	Present
381	G2-Na+-oxi	Present	Present
403	G2-Na+-Na+-oxi	ND	Present
397	G2 Na+-oxi-oxi	Present	Present
DP3			
527	G3-Na+	ND	Present
543	G3-Na+-oxi	ND	ND
565	G3-Na+-Na+-oxi	Present	Present
559	G3 Na+-oxi-oxi	Present (minor) Present	Present
DP4			
689	G4-Na+	Present	ND
705	G4-Na+-oxi	Present	Present
727	G4-Na+-Na+-oxi	ND	Present
721	G4 Na+-oxi-oxi	Present	Present
DP5			
851	G5-Na+	Present	Present
867	G5-Na+-oxi	Present	Present
889	G5-Na+-Na+-oxi	Present	Present
883	G5 Na+-oxi-oxi	Present	Present
DP6			
1013	G6-Na+	Present	Present
1029	G6-Na+-oxi	Present	Present
1051	G6-Na+-Na+-oxi	Present	Present
1045	G6 Na+-oxi-oxi	ND	Present
DP7			
1175	G7-Na+	Present	Present
1191	G7-Na+-oxi	Present	Present
1213	G7-Na+-Na+-oxi	Present	Present
1207	G7 Na+-oxi-oxi	Present	Present
DP8			
1337	G8-Na+	Present	Present
1353	G8-Na+-oxi	Present	Present
1375	G8-Na+-Na+-oxi	Present	Present
1369	G8 Na+-oxi-oxi	Present	Present

724

725

726

727

728

729

730

731

732

733

734

735

736

737

738

739

740

741

742

743

744

745

746

Highlights

- A novel LPMO from *Malbranchea cinnamomea* was heterologously expressed in *P. pastoris*
- rPMO9A_MALCI is a promiscuous LPMO with a unique ability to cleave both glucans and pure xylans.
- MS and HPAEC analysis showed the presence of both C1 and C4 oxidised products.
- rPMO9A_MALCI acts synergistically with CelliCTec2 to hydrolyze pretreated biomass.